BMC Cancer

RESEARCH

Open Access

Inhibition of miR-325 inhibits KIF20B expression and the colorectal cancer cells' invasion & proliferation

Qi-Qi Zheng[1] and Wen-Feng Lin[2*]

Abstract

Objective This study aimed to investigate the effect of miR-325 on KIF20B expression and its role in the invasion and proliferation of colorectal cancer cells.

Methods Colorectal cancer HCT116 cells were cultured and transfected with a miR-325 inhibitor. KIF20B expression was assessed using quantitative polymerase chain reaction (qPCR) and western blotting. Cell proliferation was assessed with the Cell Counting Kit-8 (CCK8) assay, while invasion was evaluated using Transwell and scratch wound healing assays. The expression levels of the invasion-related proteins Matrix Metalloproteinase-2 (MMP-2) and MMP-9 were also analyzed.

Results The q-PCR and western blot results demonstrated that KIF20B expression was significantly reduced by miR-325 inhibition. The CCK8 assay revealed that miR-325 inhibition decreased cell proliferation. Furthermore, Transwell and Scratch Wound Healing assays showed that miR-325 inhibition suppressed the invasive capacity of colorectal cancer cells. The inhibition of miR-325 also led to decreased expression levels of MMP-2 and MMP-9.

Conclusion miR-325 inhibition effectively suppresses KIF20B expression, reducing the invasion and proliferation of colorectal cancer cells, suggesting miR-325 as a potential therapeutic target.

Keywords Colorectal cancer, KIF20B, Invasion, Proliferation

Introduction

Colorectal cancer (CRC) is currently the fourth leading cause of cancer-related mortality worldwide, responsible for nearly 900,000 deaths annually [1], accounting for approximately 10% of all cancer-related deaths globally [2]. It is the second most commonly diagnosed cancer in females and the third in males. About 25% of colorectal cancer patients present with hepatic metastases at diagnosis, and approximately 50% will develop hepatic metastases within three years post-surgery [3]. Therefore, understanding the regulatory mechanisms driving metastatic progression is crucial for improving patient outcomes.

*Correspondence:
Wen-Feng Lin
linwenfeng1235@sina.com
[1]Department of Infectious Diseases and Hepatology, The First Affiliated Hospital of Wenzhou Medical University, Wenzhou 325000, Zhejiang Province, P.R. China
[2]Department of Gastroenterology and Hepatology, The First Affiliated Hospital of Wenzhou Medical University, Nanbaixiang, Ouhai District, Wenzhou City, Wenzhou City 325000, Zhejiang Province, P.R. China

Kinesin family proteins (KIFs) are motor proteins that transport cellular cargo along microtubules, using Adenosine Triphosphate (ATP) to generate motility [4]. KIFs play a key role in various biological processes, including cell division [5], intracellular transport [4], microtubule stabilization [6], and microtubule depolymerizers [6]. Numerous studies have suggested that the abnormal expression of KIFs can promote various cancer progression [7–10]. KIF20B, in particular, not only play a physiological role in mitosis but also contributes to the development of solid tumors such as pancreatic cancer [11], renal cell carcinoma [12] and hepatic carcinoma [13]. In a previous study [14], we found that KIF20B expression in CRC tissues is correlated with patient prognosis. Additionally, our findings demonstrated that KIF20B is crucial for enhancing EMT and the formation of pseudopod-like protrusions in CRC cells activated by Gli1.

To date, many biomarkers for various cancers have been identified [15–17]. MicroRNAs (miRNAs) have emerged as reliable biomarkers for the prognosis and progression of colorectal cancer, given their critical roles in tumor growth [18]. Recently, there has been increasing interest in the regulatory roles of miRNAs in biological processes, particularly in tumor cells, such as differentiation, cell cycle regulation, apoptosis, and proliferation [19]. These miRNAs are often dysregulated in cancers. For example, miR-1236-3p inhibits the proliferation, invasion, and migration of colorectal cancer cells by targeting Doublecortin Like Kinase 3 (DCLK3) and blocking epithelial-mesenchymal transition [20]. miR-570 exerts tumor-suppressive effects in CRC patients, with its overexpression inhibiting cell proliferation, migration, and invasion [21]. Furthermore, miR-186-3p inhibits colorectal cancer cell proliferation and invasion by targeting Keratin 18 (KRT18) and suppressing the Mitogen-Activated Protein Kinase (MAPK) pathway, promoting apoptosis in colorectal cancer cells [22]. miR-325 has been reported to reduce Sterol Regulatory Element Binding Transcription Factor 1 (SREBF1) expression by inhibiting KDM1A, thereby blocking the PPARγ-LXR-ABCA1 pathway and preventing atherosclerosis progression [23]. In addition, miR-325 is implicated in the progression of nasopharyngeal carcinoma [24].

In this study, we investigated the effect of miR-325 inhibition on KIF20B expression. Furthermore, we explored how miR-325 inhibition affected the proliferation and invasion of colorectal cancer cells.

Methods and materials

Cell culturing

Human CRC cell lines HCT116 were obtained from the Shanghai Institute of Biochemistry and Cell Biology, Chinese Academy of Science (Shanghai, China). The cells were cultured in Dulbecco's Modified Eagle Medium (DMEM) supplemented with 10% fetal bovine serum, 100 U/mL penicillin, and 100 μg/mL streptomycin, and incubated in a humidified atmosphere at 37 °C with 5% CO_2.

Cell transfection

HCT116 colorectal cancer cells were transfected with miR-325 inhibitor or negative control (NC) oligonucleotides, which were purchased from Sangon Biotech (Shanghai, Co., Ltd.). Transfection was carried out using Lipofectamine 2000 (Invitrogen, Thermo Fisher Scientific, CA, USA) following the manufacturer's protocol. Briefly, cells were seeded into 6-well plates at a density of 2×10^5 cells per well and allowed to adhere overnight in DMEM supplemented with 10% fetal bovine serum (FBS) at 37 °C with 5% CO2.

For each well, 5 μL of Lipofectamine 2000 was diluted in 250 μL of serum-free DMEM, and 100 pmol of miR-325 inhibitor or NC was diluted in a separate 250 μL of serum-free DMEM. The two solutions were mixed gently and incubated at room temperature for 20 min to allow for complex formation. The mixture was then added to the cells, and they were incubated for 6 h. After the transfection period, the medium was replaced with fresh DMEM containing 10% FBS, and cells were cultured for an additional 48 h before being harvested for further analysis.

RNA extraction and quantitative real-time PCR

Total RNA was extracted from HCT116 cells using TRIzol reagent (Takara, Japan) following the manufacturer's instructions. The concentration and purity of the RNA were determined using a Nanodrop spectrophotometer. Subsequently, 1 μg of total RNA was reverse-transcribed into complementary DNA (cDNA) using the PrimeScript RT reagent kit (Takara, Japan) according to the manufacturer's protocol.

Quantitative real-time PCR (qPCR) was performed using SYBR-Green (Takara, Japan) on an Applied Biosystems StepOnePlus Real-Time PCR system (Thermo Fisher Scientific, USA). The PCR program was as follows: an initial denaturation step at 95 °C for 30 s, followed by 40 amplification cycles of 95 °C for 5 s, 60 °C for 30 s, and 72 °C for 30 s. After amplification, a melting curve analysis was performed from 60 °C to 95 °C with a ramp rate of 0.3 °C per second to verify the specificity of the PCR products.

Each reaction was carried out in triplicate in a 20 μL reaction volume containing 10 μL of SYBR-Green mix, 1 μL of cDNA, 0.4 μL of each forward and reverse primer (10 μM), and 8.2 μL of RNase-free water. GAPDH was used as the internal reference gene. Relative gene expression levels were calculated using the $2^{-\Delta\Delta Ct}$ method. The primer sequences used for qRT-PCR are listed in Table 1.

Table 1 Primer sequences

Gene	Primer
miR-325 forward 5′–3	5′-TGACGGATTGATGTTAGAGGGATG-3′
miR-325 stem-loop primer 5′–3	5′-CGGAAAGCCCTAGCAGGATAATCT-3′
KIF20B sense	5′-CGGACAGGATTGACAGATTGATAGC-3′
KIF20B antisense	5′-TGCCAGAGTCTCGTTCGTTATCG-3′
GAPDH forward	5′-CGTGGGCCGCCCTAGGCACCA–3′
GAPDH reverse	5′-TTGGCTTAGGGTTCAGGGGGG–3′

Western blotting

Total protein was extracted from HCT116 cells 48 h post-transfection using RIPA lysis buffer (Beyotime, China) containing a protease inhibitor cocktail (Kangchen, China). Cells were harvested and lysed on ice for 30 min, followed by centrifugation at 12,000 rpm for 15 min at 4 °C to remove cell debris. The supernatant was collected, and the protein concentration was determined using the bicinchoninic acid (BCA) protein assay kit (Pierce Biotechnology, USA).Equal amounts of protein (20–30 μg per sample) were denatured in SDS loading buffer by boiling at 95 °C for 5 min, and then separated by 10% SDS-PAGE (sodium dodecyl sulfate-polyacrylamide gel electrophoresis). Proteins were transferred to nitrocellulose membranes (Millipore, USA) using a wet transfer system at 100 V for 90 min at 4 °C.

After transfer, membranes were blocked with 5% non-fat milk in Tris-buffered saline with 0.1% Tween-20 (TBS-T) for 1 h at room temperature to prevent nonspecific binding. The membranes were then incubated overnight at 4 °C with primary antibodies against KIF20B (1:1000 dilution, Abcam, UK), MMP-2 (1:1000 dilution, Cell Signaling Technology, USA), MMP-9 (1:1000 dilution, Cell Signaling Technology, USA), and β-actin (1:5000 dilution, Proteintech, USA), which served as a loading control.

Following primary antibody incubation, the membranes were washed three times with TBS-T and incubated with horseradish peroxidase (HRP)-conjugated secondary antibodies (1:5000 dilution, Cell Signaling Technology, USA) for 1 h at room temperature. After secondary antibody incubation, the membranes were washed again three times with TBS-T. Protein bands were visualized using an enhanced chemiluminescence (ECL) detection kit (Thermo Fisher Scientific, USA), and images were captured using a chemiluminescent imaging system.

Densitometric analysis was performed using ImageJ software to quantify the relative protein expression levels. The expression of target proteins (KIF20B, MMP-2, MMP-9) was normalized to β-actin, and the results.

Densitometric analysis (relative or adjusted density)

This method is commonly used for Western blotting, where the intensity of the bands on the gel is measured and compared. Steps:

1. Run Your Samples and Standards: Prepare your samples (e.g., HCT116 cell lysates) and load them onto the gel. Include a known concentration of a standard protein (e.g., BSA) to create a standard curve for quantification.
2. Transfer and Probe for Target Protein: After electrophoresis, transfer the proteins to a membrane (e.g., PVDF or nitrocellulose), and probe with the primary and secondary antibodies. The target proteins (e.g., KIF20B, MMP-2, MMP-9) and the internal control (e.g., β-actin) will be detected.
3. Image the Membrane: After detection (e.g., chemiluminescence or fluorescence), capture an image of the membrane using a gel imaging system (e.g., Bio-Rad Chemidoc or Odyssey scanner).
4. Quantify Band Intensities: Using software (such as ImageJ, Bio-Rad Image Lab, or Odyssey), measure the intensity of each band in the target protein (KIF20B, MMP-2, MMP-9) and β-actin.
   Relative Density (RD): The relative density is the intensity of the target protein divided by the intensity of the internal control (β-actin).
   Adjusted Density (Adj. Density): Adjusted density is calculated by normalizing the band intensity to β-actin and correcting for any variations in background. This is the intensity of the target protein band minus the background density, divided by the intensity of the β-actin band on the same membrane.
   The formula for relative density is:
   Relative Density (RD) = Intensity of target protein/Intensity of β-actin.
   For adjusted density:
   Adjusted Density (Adj. Density)=(Intensity of target protein – Background)/Intensity of β-actin.
5. Use a Standard Curve for Quantification (Optional): If you are quantifying the absolute concentration of your protein, use a standard curve. This involves loading known concentrations of a standard protein (e.g., BSA or a recombinant protein) alongside your samples. From the densitometric analysis of the standard curve, you can calculate the concentration of your unknown samples by comparing the relative density of your target protein to that of the standards.

Transwell invasion test

The invasive capacity of HCT116 cells was assessed using a Transwell invasion assay. Transwell inserts with an 8 μm pore size (Corning, USA) were pre-coated with

50 µL of Matrigel (diluted 1:8 in serum-free DMEM; BD Biosciences, USA) and allowed to solidify at 37 °C for 2 h.

HCT116 cells were trypsinized, counted, and resuspended in serum-free DMEM. A total of 200 µL of the cell suspension (containing 1×10^5 cells) was added to the upper chamber of each insert. The lower chamber was filled with 800 µL of DMEM supplemented with 20% fetal bovine serum (FBS) as a chemoattractant.

Cells were incubated at 37 °C with 5% CO2 for 24 h. After incubation, non-invading cells on the upper surface of the membrane were carefully removed using a cotton swab. The cells that had invaded through the Matrigel and migrated to the lower surface of the membrane were fixed with 4% paraformaldehyde for 10 min and stained with 0.1% crystal violet for 30 min.

The inserts were washed with PBS, and the number of invading cells was counted under a light microscope in five randomly selected fields. The invasion assay was performed in triplicate, and the results are presented as the mean ± SEM.

Scratch wound healing assay

The migration ability of HCT116 cells was assessed using a wound healing (scratch) assay. Cells were seeded in 6-well plates and cultured in DMEM supplemented with 10% fetal bovine serum (FBS) at 37 °C with 5% CO2 until they reached 80–90% confluency.

Once the desired confluence was achieved, a sterile 200 µL pipette tip was used to create a straight scratch (wound) across the monolayer of cells. The cells were then washed twice with PBS to remove debris and floating cells. After washing, the medium was replaced with serum-free DMEM to prevent cell proliferation and focus on cell migration.

Images of the wound area were captured immediately after scratching (0 h) and after 24 h using an inverted microscope. The migration of cells into the wound area was quantified by measuring the width of the wound at several random points. The experiment was performed in triplicate, and the results are presented as the mean percentage of wound closure ± SEM.

Statistical analysis

Statistical analysis was performed using Prism Software 9.0 (GraphPad, La Jolla, USA). Data were expressed as Mean ± SEM. Comparisons between groups were made using one-way ANOVA, and statistical significance was set at $p < 0.05$.

Result

miR-325 inhibition reduces KIF20B expression

To investigate the regulation of KIF20B by miR-325, HCT116 cells were transfected with a miR-325 inhibitor, and KIF20B expression was assessed using qPCR and western blotting. The results demonstrated that miR-325 inhibition significantly reduced KIF20B expression (Figs. 1A and B and 2A, and 2B).

miR-325 inhibition suppresses HCT116 cell proliferation

The effect of miR-325 inhibition on the proliferation of HCT116 cells was assessed using the CCK8 assay. The results showed that miR-325 inhibition significantly reduced the proliferation ability of HCT116 cells (Fig. 1C).

miR-325 expression reduces the invasive ability of HCT116 cells

The effect of miR-325 inhibition on the invasive capacity of HCT116 cells was evaluated using Transwell and scratch wound healing assays. The results indicated that miR-325 inhibition significantly reduced the invasive ability of HCT116 cells (Fig. 2E-G). Furthermore, western blot and ELISA assays showed that mir-325 inhibition decreased the expression levels of MMP-2 and MMP-9, both of which are associated with cell invasion. (Figure 2A, C and D).

Discussion

In 2020, approximately 1.2 million new cases of colorectal cancer were diagnosed, resulting in 600,000 deaths worldwide [25]. Colorectal cancer ranks as the fifth most common cancer in terms of both incidence and mortality. While 90% of patients with localized CRC survive for five years, the survival rate decreases to 71% and 14% for patients with regional or distant disease, respectively [26]. Drug resistance contributes to the high relapse rate observed in about 50% of patients with advanced colorectal cancer, and the five-year survival rate for these patients drops to less than 10% [27, 28]. Moreover, 25% of patients present with liver metastases at diagnosis, and 50% will develop liver metastases within three years following surgery cancer-related [29]. Metastasis is the leading cause of mortality.

miRNAs are small non-coding RNAs that regulate the translation of target mRNAs by binding to complementary regions in the 3'-UTR [30]. miRNAs are involved in numerous biological processes, including cell growth, proliferation, apoptosis, and differentiation [31]. They can function as either tumor suppressors or oncogenes, depending on their expression levels [21, 32]. For example, miR-325 has been identified as a tumor suppressor in several cancers, including non-small cell lung cancer, where it inhibits cell invasion and proliferation [33]. miR-325 has also been associated with melanoma and breast cancer, where it regulates cell proliferation, invasion, and migration [34, 35]. Additionally, miR-325 has been shown to activate the HSPA12B/PI3K/AKT/Bcl-2 pathway,

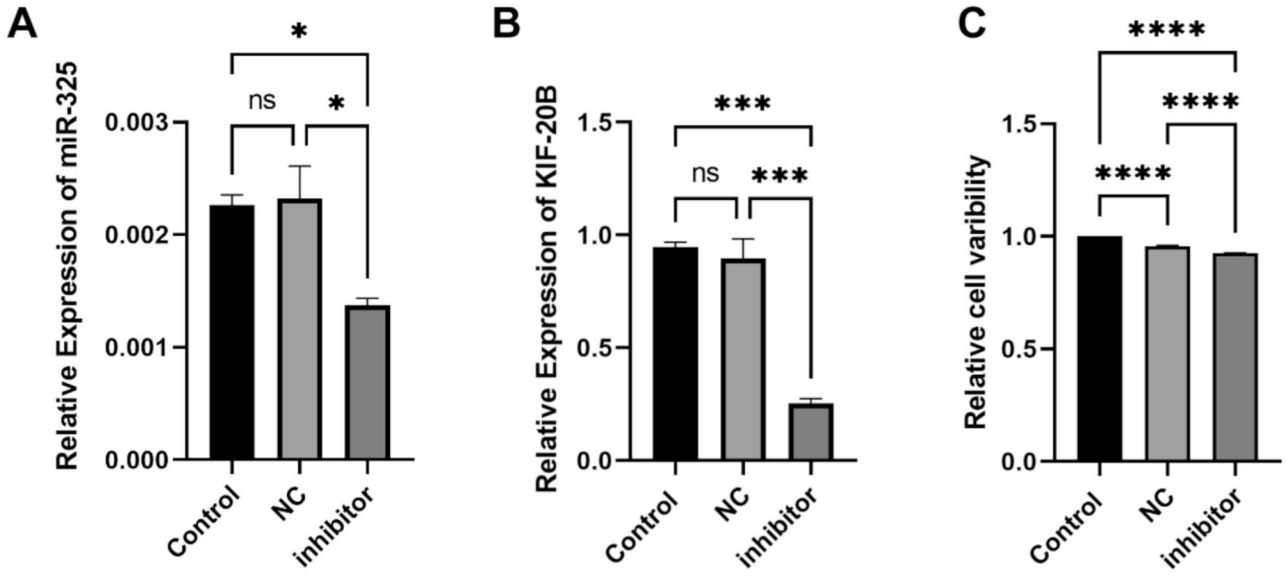

Fig. 1 (**A**) q-PCR detection of miR-325 expression results. Total RNA was extracted 48 h post-transfection, and qPCR was performed using SYBR-Green detection. The data are presented as the mean ± SEM from three independent experiments. miR-325 inhibition significantly reduced KIF20B mRNA levels compared to the NC group ($p < 0.05$, $n = 3$). (**B**) q-PCR detection of KIF20B expression results. Quantitative PCR (qPCR) analysis of KIF20B mRNA expression in HCT116 cells transfected with miR-325 inhibitor or negative control (NC). Total RNA was extracted 48 h post-transfection, and qPCR was performed using the SYBR-Green method. The relative expression of KIF20B was normalized to GAPDH as an internal control, and results are expressed as fold changes relative to the NC group. miR-325 inhibition significantly downregulated KIF20B mRNA levels compared to the NC group ($p < 0.05$, $n = 3$). (**C**) CCK8 experimental results. Cell proliferation assay of HCT116 cells transfected with miR-325 inhibitor or negative control, measured using the CCK8 assay at 24, 48, and 72 h post-transfection. Absorbance at 450 nm was measured to assess cell viability. miR-325 inhibition significantly reduced cell proliferation at all time points compared to the NC group ($p < 0.01$, $n = 3$). Results are presented as the mean ± SEM from three independent experiments. *$P < 0.05$, **$P < 0.01$, ***$P < 0.001$, ****$P < 0.0001$

sensitizing colorectal cancer cells to oxaliplatin-induced cytotoxicity [36].

One possible mechanism through which miR-325 regulates KIF20B could be by binding directly to the 3'-UTR of KIF20B mRNA, leading to its degradation or translational repression. This mechanism is commonly observed in miRNA-mediated gene regulation, and further studies using miRNA target prediction tools and luciferase reporter assays could help confirm whether KIF20B is a direct target of miR-325. Additionally, it would be valuable to explore whether other downstream pathways, such as MAPK or Wnt, are also affected by miR-325's regulation of KIF20B, as these pathways are known to play roles in colorectal cancer progression.

KIF20B, a member of the kinesin superfamily (also known as MPHOSPH1), is a microtubule-associated protein that plays a critical role in cell division, particularly during mitosis [37]. In addition to its physiological role, KIF20B has been implicated in the progression of several cancers, including hepatocellular carcinoma [38] and breast cancer [39].

In this study, we demonstrated that miR-325 regulates KIF20B expression in colorectal cancer. the inhibition of miR-325 reduced both the proliferation and invasion of these cells, suggesting that miR-325 may serve as a potential therapeutic target for the treatment of colorectal cancer. Our findings are consistent with previous studies on miRNAs in colorectal cancer. For instance, miR-570 and miR-186-3p suppress CRC progression by targeting key regulatory proteins [40, 41]. These studies, along with our findings, underscore the importance of miRNAs in the regulation of key proteins such as KIF20B in colorectal cancer. However, our study is the first to demonstrate a direct regulatory link between miR-325 and KIF20B in CRC, providing new insights into miRNA-mediated regulation in this context.

Nedaeinia et al. explored the therapeutic potential of targeting miR-21, a well-established oncomiR in colorectal cancer, demonstrating that its inhibition using LNA-anti-miR-21 reduced cell proliferation, induced apoptosis, and suppressed metastatic potential [42]. Similarly, the present study found that inhibiting miR-325 led to decreased KIF20B expression, resulting in the suppression of colorectal cancer cell proliferation and invasion. Both studies highlight miRNA inhibition as an effective strategy for reducing tumor progression.

Although both studies emphasize the role of miRNA inhibition, the mechanisms underlying these effects differ. In the case of miR-21, Nedaeinia et al. identified PDCD4 as a key downstream target, playing a crucial role in apoptosis and metastasis [43]. On the other hand, this study focuses on miR-325, which regulates KIF20B,

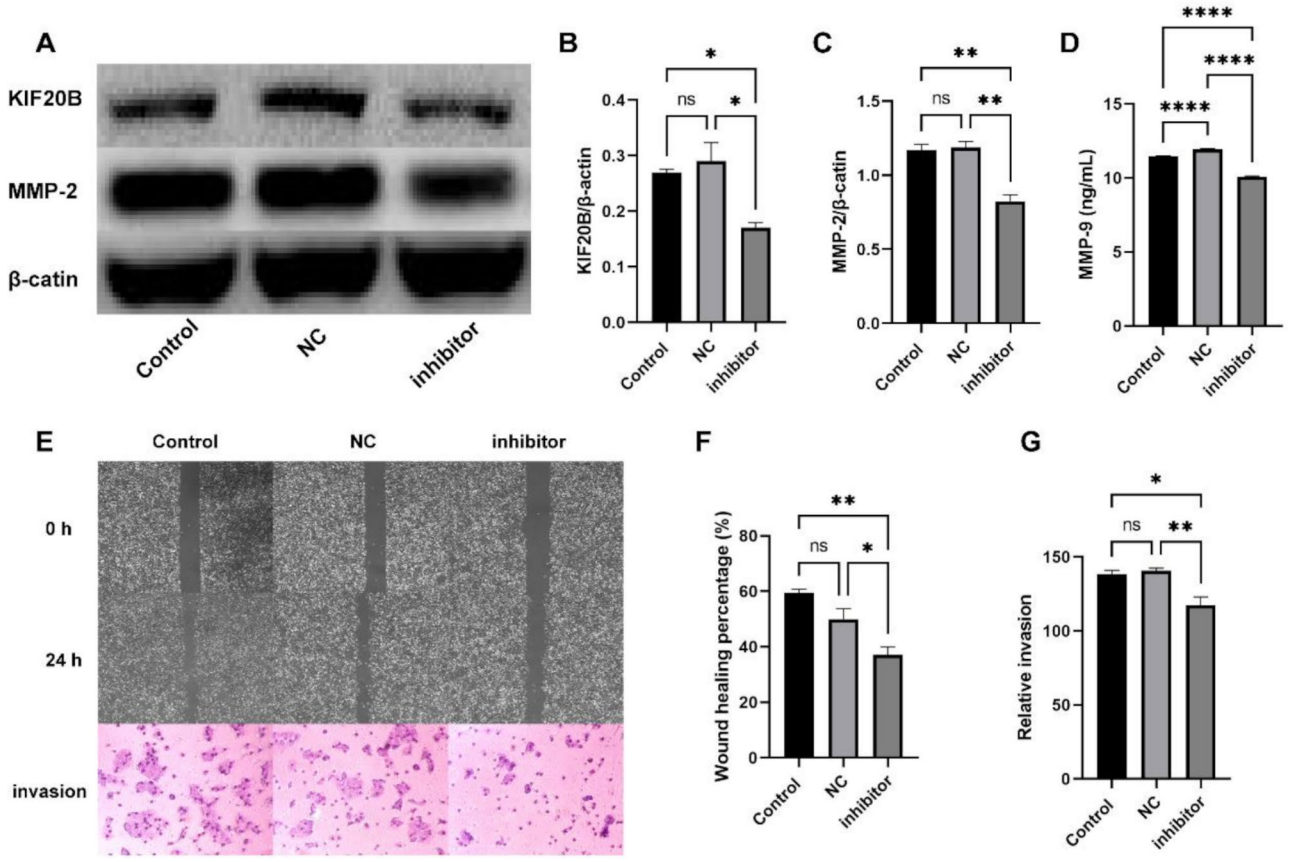

Fig. 2 (**A**) Western blot analysis of MMP-2 protein levels in HCT116 cells transfected with miR-325 inhibitor or negative control. Protein was extracted 48 h post-transfection, and MMP-2 levels were detected using specific antibodies. β-actin was used as a loading control. Densitometric analysis showed that miR-325 inhibition significantly reduced MMP-2 expression compared to the NC group ($p < 0.05$, $n = 3$). (**B**) Western blot analysis of KIF20B protein expression in HCT116 cells transfected with miR-325 inhibitor or negative control (NC). Total protein was extracted 48 h post-transfection, separated by SDS-PAGE, and transferred to nitrocellulose membranes. KIF20B protein levels were detected using specific antibodies, with β-actin serving as the loading control. The relative expression of KIF20B was quantified by densitometric analysis using ImageJ software. miR-325 inhibition significantly reduced KIF20B protein levels compared to the NC group ($p < 0.05$, $n = 3$). (**C**) Western blot analysis of MMP-2 protein expression in HCT116 cells transfected with miR-325 inhibitor or negative control (NC). Total protein was extracted 48 h post-transfection, separated by SDS-PAGE, and transferred to nitrocellulose membranes. MMP-2 protein levels were detected using specific antibodies, with β-actin serving as the loading control. Densitometric analysis was performed using ImageJ software to quantify the relative expression of MMP-2. miR-325 inhibition significantly reduced MMP-2 protein levels compared to the NC group ($p < 0.05$, $n = 3$). (**D**) Western blot analysis of MMP-9 protein expression in HCT116 cells transfected with miR-325 inhibitor or negative control (NC). Total protein was extracted 48 h post-transfection, separated by SDS-PAGE, and transferred to nitrocellulose membranes. MMP-9 protein levels were detected using specific antibodies, with β-actin serving as the loading control. Densitometric analysis was conducted using ImageJ software to quantify the relative expression of MMP-9. miR-325 inhibition significantly reduced MMP-9 protein levels compared to the NC group ($p < 0.05$, $n = 3$). (**E**) Scratch wound healing assay to evaluate cell migration in HCT116 cells transfected with miR-325 inhibitor or negative control (NC). A scratch was made in a confluent monolayer of HCT116 cells using a pipette tip, and images were taken at 0 and 24 h post-scratch. The wound closure was quantified to assess cell migration capacity. miR-325 inhibition significantly reduced wound closure compared to the NC group, indicating a suppression of cell migration ($p < 0.05$, $n = 3$). Results are presented as the mean ± SEM from three independent experiments. (**F**) Transwell invasion assay assessing the invasive ability of HCT116 cells transfected with miR-325 inhibitor or negative control (NC). Cells were seeded into the upper chambers of Transwell inserts coated with Matrigel. After 24 h, cells that invaded through the Matrigel were fixed, stained with crystal violet, and counted under a microscope. miR-325 inhibition significantly reduced the number of invaded cells compared to the NC group ($p < 0.05$, $n = 3$). Results are presented as the mean ± SEM from three independent experiments. (**G**) Transwell invasion assay demonstrating the effect of miR-325 inhibition on the invasive ability of HCT116 colorectal cancer cells. Cells were transfected with miR-325 inhibitor or negative control (NC) and seeded into the upper chambers of Transwell inserts pre-coated with Matrigel. After 24 h of incubation, cells that had invaded through the Matrigel to the lower chamber were fixed, stained with crystal violet, and counted in five randomly selected fields under a microscope. miR-325 inhibition significantly reduced the number of invading cells compared to the NC group ($p < 0.05$, $n = 3$). Results are presented as the mean ± SEM from three independent experiments. *$P < 0.05$, **$P < 0.01$, ***$P < 0.001$, ****$P < 0.0001$

a protein essential for mitosis and cell division. Furthermore, while Nedaeinia et al. investigated the influence of exosomal miRNAs in CAFs and their impact on the tumor microenvironment [44], the current research centers on the intracellular mechanisms within colorectal cancer cells.

Despite these mechanistic differences, both studies underscore the therapeutic potential of miRNA

inhibition in colorectal cancer, targeting distinct but complementary pathways. Future research may explore whether miR-325 also plays a role in the tumor microenvironment, similar to the role of miR-21 identified by Nedaeinia et al. in their studies [44].

Conclusion

This study identified miR-325 as a regulator of KIF20B expression in HCT116 colorectal cancer cells. The inhibition of miR-325 significantly reduced the invasive and proliferative capacities of these cells, providing evidence that miR-325 could be a promising therapeutic target for colorectal cancer treatment. Further studies are necessary to elucidate the underlying mechanisms by which miR-325 regulates KIF20B, and these findings will be explored through animal and molecular biology experiments.

Supplementary Information

The online version contains supplementary material available at https://doi.org/10.1186/s12885-025-13759-z.

Supplementary Material 1

Acknowledgements

Thanks for the financial supported of Wenzhou Science and Technology Project (The role and mechanism of cell protrusion protein KIF20B in the metastasis of colon cancer), NO. Y20180098.

Author contributions

We declare that all the listed authors have participated actively in the study and all meet the requirements of the authorship. Dr. WFL designed the study and wrote the paper, Dr. QQZ managed the literature searches and analyses. All authors reviewed the manuscript.

Funding

This project was supported by Wenzhou Science and Technology Project (The role and mechanism of cell protrusion protein KIF20B in the metastasis of colon cancer), NO. Y20180098.

Data availability

The datasets used or analyzed during the current study are available from the corresponding author on reasonable request.

Declarations

Statement of ethics

Not Applicable.

Consent for publication

The work described has not been published previously.

Conflict of interest

The authors have no conflicts of interest to declare.

Received: 13 August 2024 / Accepted: 18 February 2025
Published online: 14 April 2025

References

1. Dekker E, Tanis PJ, Vleugels JLA, et al. Colorectal cancer [J]. Lancet (London England). 2019;394(10207):1467–80.
2. Bray F, Ferlay J, Soerjomataram I, et al. Global cancer statistics 2018: GLOBOCAN estimates of incidence and mortality worldwide for 36 cancers in 185 countries [J]. Cancer J Clin. 2018;68(6):394–424.
3. Desantis CE, Lin CC, Mariotto AB, et al. Cancer treatment and survivorship statistics, 2014 [J]. Cancer J Clin. 2014;64(4):252–71.
4. Hirokawa N, Noda Y, Tanaka Y, et al. Kinesin superfamily motor proteins and intracellular transport [J]. Nat Rev Mol Cell Biol. 2009;10(10):682–96.
5. Zhao K, Li X, Feng Y, Wang J, Yao W. The role of Kinesin family members in hepatobiliary carcinomas: from bench to bedside [J]. Biomark Res. 2024;12(1):30.
6. Wordeman L. Microtubule-depolymerizing kinesins [J]. Curr Opin Cell Biol. 2005;17(1):82–8.
7. Jungwirth G, Yu T, Moustafa M et al. Identification of KIF11 as a novel target in meningioma [J]. Cancers, 2019, 11(4).
8. Ni S, Li J, Qiu S, et al. KIF21B expression in osteosarcoma and its regulatory effect on osteosarcoma cell proliferation and apoptosis through the PI3K/AKT pathway [J]. Front Oncol. 2020;10:606765.
9. Yang Y, Gao L, Weng NN, et al. Identification of novel molecular therapeutic targets and their potential prognostic biomarkers among Kinesin superfamily of proteins in pancreatic ductal adenocarcinoma [J]. Front Oncol. 2021;11:708900.
10. Gifford V, Woskowicz A, Ito N, et al. Coordination of two Kinesin superfamily motor proteins, KIF3A and KIF13A, is essential for pericellular matrix degradation by membrane-type 1 matrix metalloproteinase (MT1-MMP) in cancer cells [J]. Matrix Biology: J Int Soc Matrix Biology. 2022;107:1–23.
11. Chen J, Zhao CC, Chen FR et al. KIF20B Promotes Cell Proliferation and May Be a Potential Therapeutic Target in Pancreatic Cancer [J]. Journal of oncology. 2021;2021:5572402.
12. Li G, Xie ZK, Zhu DS, et al. KIF20B promotes the progression of clear cell renal cell carcinoma by stimulating cell proliferation [J]. Journal of cellular physiology; 2019.
13. Liu X, Li Y, Zhang X, et al. Inhibition of Kinesin family member 20B sensitizes hepatocellular carcinoma cell to microtubule-targeting agents by blocking cytokinesis [J]. Cancer Sci. 2018;109(11):3450–60.
14. Lin WF, Lin XL, Fu SW, et al. Pseudopod-associated protein KIF20B promotes Gli1-induced epithelial-mesenchymal transition modulated by pseudopodial actin dynamic in human colorectal cancer [J]. Mol Carcinog. 2018;57(7):911–25.
15. Sarhadi VK, Armengol G. Mol Biomarkers Cancer [J] Biomolecules, 2022, 12(8).
16. Novak D, Utikal J. New biomarkers in cancers [J]. Cancers, 2021, 13(4).
17. Toden S, Goel A. Non-coding RNAs as liquid biopsy biomarkers in cancer [J]. Br J Cancer. 2022;126(3):351–60.
18. He B, Zhao Z, Cai Q, et al. miRNA-based biomarkers, therapies, and resistance in Cancer [J]. Int J Biol Sci. 2020;16(14):2628–47.
19. Hussen BM, Hidayat HJ, Salihi A, et al. MicroRNA: A signature for cancer progression [J]. Volume 138. Biomedicine & pharmacotherapy = Biomedecine & pharmacotherapie; 2021. p. 111528.
20. Zhao Y, Zhou H, Shen J, et al. MiR-1236-3p inhibits the proliferation, invasion, and migration of colorectal cancer cells and hinders Epithelial-Mesenchymal transition by targeting DCLK3 [J]. Front Oncol. 2021;11:688882.
21. Jiang G, Zhang R, Yang X, et al. Positive correlation between miR-570 and prognosis of colorectal cancer: Inhibition of cell proliferation and invasion [J]. Clin Experimental Med. 2022;22(2):193–200.
22. Xia T, Zhang Z, Zhang X, et al. Hsa-miR-186-3p suppresses colorectal cancer progression by inhibiting KRT18/MAPK signaling pathway [J]. Cell Cycle (Georgetown Tex). 2022;21(7):741–53.
23. Pu Y, Zhao Q, Men X, et al. MicroRNA-325 facilitates atherosclerosis progression by mediating the SREBF1/LXR axis via KDM1A [J]. Life Sci. 2021;277:119464.
24. Liu D, Gong H, Tao Z, et al. LINC01515 promotes nasopharyngeal carcinoma progression by serving as a sponge for miR-325 to up-regulate CDCA5 [J]. J Mol Histol. 2021;52(3):577–87.
25. Sung H, Ferlay J, Siegel RL, et al. Global Cancer statistics 2020: GLOBOCAN estimates of incidence and mortality worldwide for 36 cancers in 185 countries [J]. Cancer J Clin. 2021;71(3):209–49.
26. Siegel RL, Miller KD, Fuchs HE, et al. Cancer statistics, 2021 [J]. Cancer J Clin. 2021;71(1):7–33.
27. Dahan L, Sadok A, Formento JL, et al. Modulation of cellular redox state underlies antagonism between oxaliplatin and cetuximab in human colorectal cancer cell lines [J]. Br J Pharmacol. 2009;158(2):610–20.
28. Siegel RL, Miller KD, Goding Sauer A, et al. Colorectal cancer statistics, 2020 [J]. Cancer J Clin. 2020;70(3):145–64.

29. Miller KD, Nogueira L, Devasia T et al. Cancer treatment and survivorship statistics, 2022 [J]. CA: a cancer journal for clinicians, 2022, 72(5): 409–36.
30. Lu TX, Rothenberg ME. MicroRNA [J]. J Allergy Clin Immunol. 2018;141(4):1202–7.
31. Ambros V. The functions of animal MicroRNAs [J]. Nature. 2004;431(7006):350–5.
32. Mao QD, Zhang W, Zhao K, et al. MicroRNA-455 suppresses the oncogenic function of HDAC2 in human colorectal cancer [J]. Brazilian J Med Biol Res = Revista Brasileira De Pesquisas Medicas E Biologicas. 2017;50(6):e6103.
33. Yao S, Zhao T, Jin H. Expression of MicroRNA-325-3p and its potential functions by targeting HMGB1 in non-small cell lung cancer [J]. Volume 70. Biomedicine & pharmacotherapy = Biomedecine & pharmacotherapie; 2015. pp. 72–9.
34. Chen X, Gao J, Yu Y, et al. LncRNA FOXD3-AS1 promotes proliferation, invasion and migration of cutaneous malignant melanoma via regulating miR-325/MAP3K2 [J]. Volume 120. Biomedicine & pharmacotherapy = Biomedecine & pharmacotherapie; 2019. p. 109438.
35. Liu Zk XH, Li X, Zhang RS, Bai JH, Zhang XF. MicroRNA-325 targets Lipocalin 15 to suppress proliferation, migration and invasion of breast cancer cells [J]. Archives of Medical Science; 2020.
36. Zhang L, Chen H, Song Y, et al. MiR-325 promotes Oxaliplatin-Induced cytotoxicity against colorectal Cancer through the HSPA12B/PI3K/AKT/Bcl-2 pathway [J]. Dig Dis Sci. 2021;66(8):2651–60.
37. Janisch KM, Mcneely KC, Dardick JM, et al. Kinesin-6 KIF20B is required for efficient cytokinetic furrowing and timely abscission in human cells [J]. Mol Biol Cell. 2018;29(2):166–79.
38. Liu X, Zhou Y, Liu X, et al. MPHOSPH1: a potential therapeutic target for hepatocellular carcinoma [J]. Cancer Res. 2014;74(22):6623–34.
39. Li TF, Zeng HJ, Shan Z, et al. Overexpression of Kinesin superfamily members as prognostic biomarkers of breast cancer [J]. Cancer Cell Int. 2020;20:123.
40. Baker JR, Vuppusetty C, Colley T, Hassibi S, Fenwick PS, Donnelly LE, Ito K, Barnes PJ. MicroRNA-570 is a novel regulator of cellular senescence and inflammaging. FASEB J. 2019;33(2):1605–16.
41. Wang Z, Sha HH, Li HJ. Functions and mechanisms of miR-186 in human cancer. Biomed Pharmacother. 2019;119:109428.
42. Nedaeinia R, Sharifi M, Avan A, et al. Locked nucleic acid anti-miR-21 inhibits cell growth and invasive behaviors of a colorectal adenocarcinoma cell line: LNA-anti-miR as a novel approach. Cancer Gene Ther. 2016;23(8):246–53.
43. Nedaeinia R, Sharifi M, Avan A, et al. Inhibition of microRNA-21 via locked nucleic acid-anti-miR suppressed metastatic features of colorectal cancer cells through modulation of programmed cell death 4. Tumour Biol. 2017;39(3):1010428317692261.
44. Nedaeinia R, Najafgholian S, Salehi R, et al. The role of cancer-associated fibroblasts and Exosomal miRNAs-mediated intercellular communication in the tumor microenvironment and the biology of carcinogenesis: a systematic review. Cell Death Discov. 2024;10(1):380.

Publisher's note